THE POTENTIAL FIELD APPROACH AND OPERATIONAL SPACE FORMULATION IN ROBOT CONTROL

Oussama Khatib
Artificial Intelligence Laboratory
Stanford University

Abstract

The paper presents a radically new approach to real-time dynamic control and active force control of manipulators. In this approach the manipulator control problem is reformulated in terms of direct control of manipulator motion in operational space, the space in which the task is originally described, rather than controlling the task's corresponding joint space motion obtained after geometric and kinematic transformation. The control method is based on the construction of the manipulator end effector dynamic model in operational space. Also, the paper presents a unique real-time obstacle avoidance method for manipulators and mobile robots based on the "artificial potential field" concept. In this method, collision avoidance, traditionally considered a high level planning problem, can be effectively distributed between different levels of control, allowing real-time robot operations in a complex environment. Using a time-varying artificial potential field, this technique has been extended to moving obstacles. A two-level control architecture has been designed to increase the system real-time performance. These methods have been implemented in the COSMOS system for a PUMA 560 robot arm. We have demonstrated compliance, contact, sliding, and insertion operations using wrist and finger sensing, as well as real-time collision avoidance with moving obstacles using visual sensing.

1. Introduction

Conventional manipulator control, providing only linear feedback compensation to control joint positions independently, cannot meet the high accuracy and performance needed in precision manipulator tasks. Addressing this problem, much research has been directed at developing and modelling the dynamic equations of joint motion. Typical models relate joint variables to generalized torques and by necessity force the resulting control scheme to have two levels:

- The first level requires coordinate transformations to convert the task description from operational space to joint space;
- The second level makes use of the arm's dynamic model to calculate generalized force commands.

This first stage of transforming the task description is time consuming and prone to problems near kinematic singularities. Additionally, dealing with the dynamic compensation problem leads to high computational complexity in real-time control. Furthermore, the very approach of joint space control is ill-suited for active force control, an ability which is crucial in robot assembly tasks.

Robot collision avoidance, on the other hand, has typically been a component of higher levels of control in hierarchical robot control systems. It has been treated as a planning problem, and research in this area has focused on the development of collision-free path planning algorithms [Moravec 1980, Lozano-Perez 1980, Chatila 1981, Brooks 1983]. These algorithms aim at providing the low level control with a path that will enable the robot to accomplish its assigned task free from any risk of collision.

From this perspective, the function of low level control is limited to the execution of elementary operations for which the paths have been precisely specified. The robot's interaction with its environment is then paced by the time-cycle of high level control, which is generally several orders of magnitude slower than the response time of a typical robot. This places limits on the robot's real-time capabilities for precise, fast, and highly interactive operations in a cluttered and evolving environment. We will show, however, that it is possible to greatly extend the function of low level control and to carry out more complex operations by coupling environment-sensing feedback with the lowest level of control.

Increasing the capability of low level control has been the impetus for the work on real-time obstacle avoidance that we discuss here. Collision avoidance at the low level of control is not intended to replace high level functions or to solve planning problems. The purpose here is to make better use of low level control capabilities in performing real-time operations. At this low level of control, the degree or *level of competence* [Brooks 1981] will remain less than that of higher level control.

The *operational space formulation* is the basis for the application of the potential field approach to robot manipulators. This formulation has its roots in the work on end-effector motion control and obstacle avoidance [Khatib, Llibre and Mampey 1978a, Khatib and Le Maitre 1978b] that we implemented for an MA23 manipulator at the Laboratoire d'Automatique de Montpellier in 1978. The operational space approach has been formalized by constructing its basic tool, the equations of motion in the operational space of the manipulator end-effector. Details of this work have been published elsewhere [Khatib 1980] (in French), and [Khatib 1983]; we will briefly review the fundamentals of the operational space formulation.

Proc. Fourth Yale Workshop on Applications of Adaptive Systems Theory
Yale University, May 1985

2. Operational Space Formulation

An *operational coordinate system* is a set x of m_0 *independent* parameters describing the manipulator end-effector position and orientation in a frame of reference R_0. For a non-redundant manipulator, these parameters form a set of configuration parameters in a domain of the operational space and constitute, therefore, a system of generalized coordinates. The kinetic energy of the holonomic articulated mechanism is a quadratic form of the generalized velocities:

$$T(x,\dot{x}) = \frac{1}{2}\dot{x}^T \Lambda(x)\dot{x}; \tag{1}$$

where $\Lambda(x)$ designates the symmetric matrix of the quadratic form, *i.e.* the kinetic energy matrix. Using the Lagrangian formalism, the end-effector equations of motion are given by:

$$\frac{d}{dt}(\frac{\partial L}{\partial \dot{x}}) - \frac{\partial L}{\partial x} = F; \tag{2}$$

where the Lagrangian $L(x,\dot{x})$ is:

$$L(x,\dot{x}) = T(x,\dot{x}) - U(x); \tag{3}$$

and $U(x)$ represents the potential energy of the gravity. F is the operational force vector. These equations can be developed [Khatib 1980, Khatib 1983] and written in the form:

$$\Lambda(x)\ddot{x} + \mu(x,\dot{x}) + p(x) = F; \tag{4}$$

where $\mu(x,\dot{x})$ represents the centrifugal and Coriolis forces, $p(x)$ the gravity forces.

The control of manipulators in operational space is based on the selection of F as a command vector. In order to produce this command, specific forces Γ must be applied with joint-based actuators. The relationship between F and the joint forces Γ is given by:

$$\Gamma = J^T(q)\,F; \tag{5}$$

where q is the vector of the n joint coordinates, and $J(q)$ the Jacobian matrix.

The extension of the operational space approach to redundant manipulators is presented in [Khatib 1980, Khatib 1983].

3. End-Effector Dynamic Decoupling

While in motion, a manipulator is subject to highly nonlinear inertial, centrifugal, Coriolis, and gravity forces. Dynamic decoupling, which is achieved by compensating for these forces, requires their evaluation using the manipulator dynamic model. Considering the complexity of these models, real-time dynamic control of manipulators has been viewed as a computationaly expensive approach. This problem is yet more acute in operational space, since the corresponding equations of motion are relatively more complex than those of joint motion.

Addressing this problem, we designed a two-level control system architecture based on isolating the configuration dependent coefficients in the dynamic model. The load of real-time computation of these coefficients can then be paced by the rate of configuration changes, which is much lower than that of the mechanism dynamics.

Using the dynamic model (4), the decoupling of the end-effector motion in operational space is achieved by:

$$F = \Lambda(x)F^* + \mu(x,\dot{x}) + p(x); \tag{6}$$

where F^* represents the command vector of the decoupled end-effector, which becomes equivalent to a *single unit mass*. Let $[\dot{q}\dot{q}]$ and $[\dot{q}^2]$ be:

$$\begin{aligned}[\dot{q}\dot{q}] &= [\dot{q}_1\dot{q}_2\ \dot{q}_1\dot{q}_3 \cdots \dot{q}_{n-1}\ \dot{q}_n]^T; \\ [\dot{q}^2] &= [\dot{q}_1^2\ \dot{q}_2^2 \cdots \dot{q}_n^2]^T.\end{aligned} \tag{7}$$

The joint torque vector corresponding to the operational space command vector (6) can be developed [Khatib 1980, Khatib 1983] following the structure:

$$\Gamma = J^T(q)\Lambda(q)F^* + \tilde{B}(q)[\dot{q}\dot{q}] + \tilde{C}(q)[\dot{q}^2] + g(q); \tag{8}$$

$\tilde{B}(q)$, $\tilde{C}(q)$, and $g(q)$ are the $n \times n(n-1)/2$, $n \times n$, and $n \times 1$ matrices of the joint forces under the mapping into joint space of the end-effector Coriolis, centrifugal, and gravity forces, respectively.

The dynamic decoupling of the end-effector can thus be obtained using the configuration dependent dynamic coefficients $\Lambda(q)$, $\tilde{B}(q)$, $\tilde{C}(q)$ and $g(q)$.

Furthermore, the rate of computation of the end-effector position, a costly step since it involves evaluations of the manipulator geometric model, can be reduced by integrating an operational position estimator into the control system. Finally, the control system has the following architecture:

- A low rate *parameter evaluation level*: updating the end-effector dynamic coefficients, the Jacobian matrix, and the geometric model.
- A high rate *servo control level*: computing the command vector using the estimator and the updated dynamic coefficents.

4. Active Force Control

In previous approaches [Craig and Raibert 1979, Salisbury 1980], the active force control problem has been treated within the frame of a joint space control system. However, the wrist or finger sensing, end-effector desired contact forces, and end-effector stiffness and dynamics involved in this problem are closely linked to the operational space. Active force control can be naturally integrated into the operational space control system by simply incorporating it into the operational force command vector. By decoupling the end-effector motion, compliance in a given direction in the operational space is directly controlled by the position gain matrix. Active force control in a given direction is then simply achieved by setting the end-effector stiffness in that direction to zero and selecting the corresponding force servo using the selection matrix S (see Figure). System stabilization is obtained by maintaining the damping ξ in both position and force control.

5. The Artificial Potential Field Approach

We present this method in the context of manipulator collision avoidance. Its application to mobile robots is straightforward. The philosophy of the artificial potential field approach can be schematically described as follows: *The manipulator moves in a field of forces. The position to be reached is an attractive pole for the end-effector, and obstacles are repulsive surfaces*

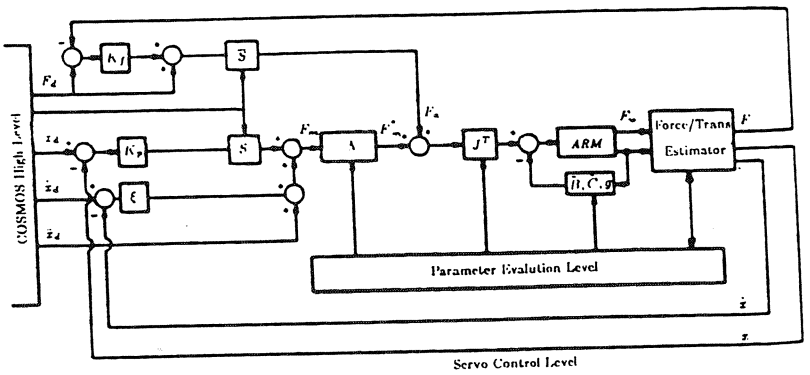

Figure 1. *Operational Space Control System Architecture*

for the manipulator parts.

Let us first consider the collision avoidance problem of a manipulator end-effector with a single obstacle $\mathcal{O}$. If x_d designates the goal position, the control of the manipulator end-effector with respect to the obstacle $\mathcal{O}$ can be achieved by subjecting it to the artificial potential field:

$$U_{art}(x) = U_{x_d}(x) + U_{\mathcal{O}}(x). \tag{9}$$

This leads to the following expression of the potential energy in the Lagrangian (3):

$$U(x) = U_{art}(x) + U_g(x); \tag{10}$$

where $U_g(x)$ represents the gravity potential energy. Using Lagrange's equations (2), and taking into account the end-effector dynamic decoupling (6), the command vector F^* of the decoupled end-effector that corresponds to applying the artificial potential field U_{art} (9) can be written as:

$$F^* = F^*_{x_d} + F^*_{\mathcal{O}}; \tag{11}$$

with:

$$\begin{aligned} F^*_{x_d} &= -grad[U_{x_d}(x)]; \\ F^*_{\mathcal{O}} &= -grad[U_{\mathcal{O}}(x)]; \end{aligned} \tag{12}$$

$F^*_{x_d}$ is an attractive force allowing the point x of the end-effector to reach the goal position x_d, and $F^*_{\mathcal{O}}$ represents a *Force Inducing an Artificial Repulsion from the Surface* of the obstacle (FIRAS, from the French), created by the potential field $U_{\mathcal{O}}(x)$. $F^*_{x_d}$ corresponds to the proportional term, *i.e.* $-k(x - x_d)$, in a conventional PD servo, where k is the position gain. The attractive potential field $U_{x_d}(x)$ is simply:

$$U_{x_d}(x) = \frac{1}{2}k(x - x_d)^2. \tag{13}$$

$U_{\mathcal{O}}(x)$ is selected such that the artificial potential field $U_{art}(x)$ is a positive continuous and differentiable function which attains its zero minimum when $x = x_d$. The articulated mechanical system subjected to $U_{art}(x)$ is stable. Asymptotic stabilization of the system is achieved by adding dissipative forces proportional to $\dot{x}$. Let ξ be the velocity gain; the forces contributing to the end-effector motion and stabilization are of the form:

$$F^*_{x_d} = -k(x - x_d) - \xi\dot{x}. \tag{14}$$

This command vector is inadequate to control the manipulator for tasks that involve large end-effector motion toward a goal position without path specification. For such a task, it is better for the end-effector to move in a straight line, with an upper speed limit.

Rewriting equation (14) leads to the following expression, which can be interpreted as specifing a desired velocity vector in a pure velocity servo-control.

$$\dot{x}_d = \frac{k}{\xi}(x_d - x). \tag{15}$$

Let V_{max} designate the assigned speed limit. The limitation of the end-effector velocity magnitude can then be obtained [Khatib, Llibre and Mampey 1978a] by:

$$F^*_{x_d} = -\xi(\dot{x} - \nu\dot{x}_d); \tag{16}$$

where:

$$\nu = min(1, \frac{V_{max}}{\sqrt{\dot{x}_d^T\dot{x}_d}}). \tag{17}$$

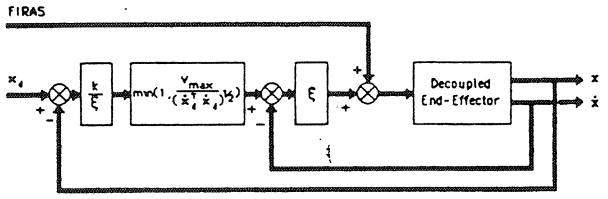

Figure 2. *End-effector Control for a Goal Position*

With this scheme, shown in Figure 2, the velocity vector $\dot{x}$ is controlled to be pointed toward the goal position while its magnitude is limited to V_{max}. The end-effector will then travel at that speed, in a straight line, except during the acceleration and deceleration segments or when it is inside the repulsive potential field regions of influence.

6. FIRAS Function

The artificial potential field $U_O(x)$ should be designed to meet the manipulator stability condition and to create at each point on the obstacle's surface a potential barrier which becomes negligible beyond that surface. Specifically, $U_O(x)$ should be a non-negative continuous and differentiable function whose value tends to infinity as the end-effector approaches the obstacle's surface. In order to avoid undesirable perturbing forces beyond the obstacle's vicinity, the influence of this potential field must be limited to a given region surrounding the obstacle.

Using analytic equations $f(x) = 0$ for obstacle description, the first artificial potential field function we used [Khatib and Le Maitre 1978b] was based on the values of the function $f(x)$:

$$U_O(x) = \begin{cases} \frac{1}{2}\eta(\frac{1}{f(x)} - \frac{1}{f(x_0)})^2, & \text{if } f(x) \leq f(x_0); \\ 0, & \text{if } f(x) > f(x_0). \end{cases} \quad (18)$$

The region of influence of this potential field is bounded by the surfaces $f(x) = 0$ and $f(x) = f(x_0)$, where x_0 is a given point in the vicinity of the obstacle and η a constant gain. This potential function can be obtained very simply in real-time since it does not require any distance calculations. However, this potential is difficult to use for asymmetric obstacles, where the separation between an obstacle's surface and equipotential surfaces can vary widely.

Using the shortest distance to an obstacle O, we have proposed [Khatib 1980] the following artificial potential field:

$$U_O(x) = \begin{cases} \frac{1}{2}\eta(\frac{1}{\rho} - \frac{1}{\rho_0})^2, & \text{if } \rho \leq \rho_0; \\ 0, & \text{if } \rho > \rho_0; \end{cases} \quad (19)$$

where ρ_0 represents the limit distance of the potential field influence and ρ, the shortest distance to the obstacle O.

Any point of the robot can be subjected to the artificial potential field. A *Point Subjected to the Potential* is called a PSP. The control of a PSP with respect to an obstacle O is achieved using the FIRAS function:

$$F^*_{(O,psp)} = \begin{cases} \eta(\frac{1}{\rho} - \frac{1}{\rho_0})\frac{1}{\rho^2}\frac{\partial \rho}{\partial x}, & \text{if } \rho \leq \rho_0; \\ 0, & \text{if } \rho > \rho_0; \end{cases} \quad (20)$$

where $\frac{\partial \rho}{\partial x}$ denotes the partial derivative vector of the distance from the PSP to the obstacle:

$$\frac{\partial \rho}{\partial x} = [\frac{\partial \rho}{\partial x}\ \frac{\partial \rho}{\partial y}\ \frac{\partial \rho}{\partial z}]^T. \quad (21)$$

Observing (6) and (11), the joint forces corresponding to $F^*_{(O,psp)}$ are obtained using the Jacobian matrix associated with this PSP. These forces are given by:

$$\Gamma_{(O,psp)} = J^T_{psp}(q)\Lambda(x)F^*_{(O,psp)}. \quad (22)$$

7. Obstacle Geometric Modelling

Obstacles are described by the composition of *primitives*. A typical geometric model base includes primitives such as a point, line, plane, ellipsoid, parallelepiped, cone, and cylinder. The first artificial potential field (18) requires analytic equations for the description of obstacles. For primitives such as a *parallelepiped*, *finite cylinder*, and *cone*, we have developed analytic equations representing envelopes which best approximate the primitives' shapes.

The surface, termed an *n-ellipsoid*, is represented by the equation:

$$(\frac{x}{a})^{2n} + (\frac{y}{b})^{2n} + (\frac{z}{c})^{2n} = 1; \quad (23)$$

and tends to a parallelepiped of dimensions (a,b,c) as n tends to infinity. A good approximation is obtained with $n = 4$, as shown in Figure 3.

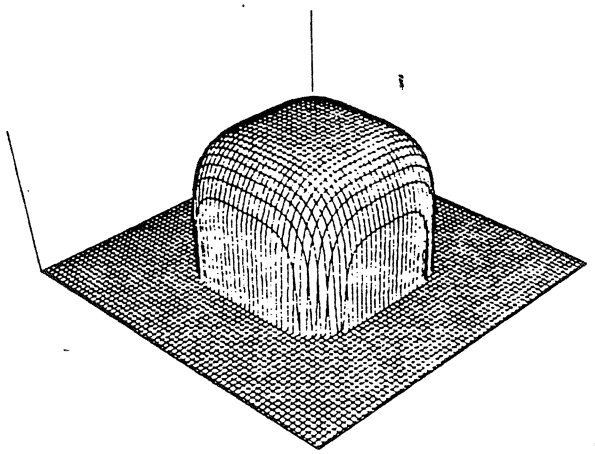

Figure 3. *An n-ellipsoid with n=4*

A cylinder of elliptical cross section (a, b) and of length $2c$ can be approximated by the so-called *n-cylinder* equation:

$$(\frac{x}{a})^2 + (\frac{y}{b})^2 + (\frac{z}{c})^{2n} = 1. \quad (24)$$

The analytic description of primitives is not necessary for the artificial potential field (19), since the continuity and differentiablity requirement is on the shortest distance to the obstacle. The primitives above, and more generally all convex primitives, comply with this requirement.

Determining the orthogonal distance to an n-ellipsoid or to an n-cylinder requires the solution of a complicated system of equations. To avoid this costly computation, a variational procedure for the distance evaluation has been developed. The distance expressions for other primitives are presented in [Khatib 1985].

8. Robot Obstacle Avoidance

An obstacle O_i is described by a set of primitives $\{P_p\}$. The superposition property (additivity) of potential fields enables the control of a given point of the manipulator with respect to this obstacle by using the sum of the relevant gradients:

$$F^*_{O_i,psp} = \sum_p F^*_{(P_p,psp)}. \quad (25)$$

Control of this point for several obstacles is obtained using:

$$F^*_{psp} = \sum_i F^*_{(O_i,psp)}. \quad (26)$$

It is also feasible to have different points on the manipulator controlled with respect to different obstacles. The resulting joint force vector is given by:

$$\Gamma_{obstacles} = \sum_j J^T_{psp_j}(q)\Lambda(x)F^*_{psp_j}. \quad (27)$$

Specifying an adequate number of PSP's enables the protection of all of the manipulator's parts. An example of a dynamic simulation for a redundant 4 *dof* manipulator operating in the plane [Khatib and Le Maitre 1978b] is shown in the display of Figure 4. The artificial potential field approach can be extended to *moving obstacles*, since stability of the mechanism persists with a continuously time-varying potential field.

The manipulator obstacle avoidance problem has been formulated in terms of *collision avoidance of links*, rather than points. Link collision avoidance is achieved by continuously controlling the link's closest point to the obstacle. At most, n PSP's then have to be considered. Additional links can be artificially introduced or the length of the last link can be extended to account for the manipulator tool or load. In an articulated chain, a link can be represented as the line segment defined by the Cartesian positions of its two neighboring joints. In a frame of reference R, a point $m(x,y,z)$ of the link bounded by $m_1(x_1,y_1,z_1)$ and $m_2(x_1,y_1,z_1)$ is described by the parametric equations:

$$\begin{aligned} x &= x_1 + \lambda(x_2 - x_1); \\ y &= y_1 + \lambda(y_2 - y_1); \\ z &= z_1 + \lambda(z_2 - z_1). \end{aligned} \quad (28)$$

The problem of obtaining the link's shortest distance to a parallelepiped can be reduced to that of finding the link's closest point to a vertex, edge, or face. The analytic expressions of the link's closest point, the distance, and its partial derivatives for a parallelepiped, cylinder and cone are given in [Khatib 1985].

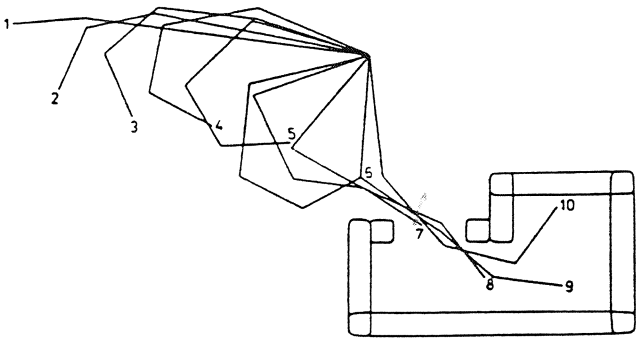

Figure 4. *Displacement of a 4 dof manipulator inside an enclosure*

9. Joint Limit Avoidance

The potential field approach can be used to satisfy the manipulator internal joint constraints. Let $\underline{q}_i$ and $\bar{q}_i$ be respectively the minimal and maximal bounds of the i^{th} joint coordinate q_i. q_i can be kept within these boundaries by creating barriers of potential at each of the hyperplanes $(q_i = \underline{q}_i)$ and $(q_i = \bar{q}_i)$. The corresponding joint forces are:

$$\Gamma_{\underline{q}_i} = \begin{cases} \eta(\frac{1}{\underline{\rho}_i} - \frac{1}{\underline{\rho}_{i(0)}})\frac{1}{\underline{\rho}_i^2}, & \text{if } \underline{\rho}_i \le \underline{\rho}_{i(0)}; \\ 0, & \text{if } \underline{\rho}_i > \underline{\rho}_{i(0)}; \end{cases} \quad (29)$$

and:

$$\Gamma_{\bar{q}_i} = \begin{cases} -\eta(\frac{1}{\bar{\rho}_i} - \frac{1}{\bar{\rho}_{i(0)}})\frac{1}{\bar{\rho}_i^2}, & \text{if } \bar{\rho}_i \le \bar{\rho}_{i(0)}; \\ 0, & \text{if } \bar{\rho}_i > \bar{\rho}_{i(0)}; \end{cases} \quad (30)$$

where $\underline{\rho}_{i(0)}$ and $\bar{\rho}_{i(0)}$ represent the distance limit of the potential field influence. The distances $\underline{\rho}_i$ and $\bar{\rho}_i$ are defined by:

$$\begin{aligned} \underline{\rho}_i &= q_i - \underline{q}_i; \\ \bar{\rho}_i &= \bar{q}_i - q_i \end{aligned} \quad (31)$$

10. Level of Competence

The potential field concept is indeed an attractive approach to the collision avoidance problem, and much research has recently been focused on its applications to robot control [Kuntze and Schill 1982, Hogan 1983, Krogh 1984]. However, the complexity of tasks that can be achieved with this approach is limited. In a cluttered environment, local minima can occur in the resultant potential field. This can lead to a stable positioning of the robot before reaching its goal. While local procedures can be designed to exit from such configurations, limitations for complex tasks will remain. This is because the approach has a *local* perspective of the robot environment.

Nevertheless, the resulting potential field does provide the global information necessary, and a collision-free path, if attainable, can be found by linking the absolute minima of the potential. Linking these minima requires, however, a computationally expensive exploration of the potential field. This goes beyond the real-time control we are concerned with here, but can be considered as an integrated part of higher level control. Work on high level collision-free path planning based on the potential field concept has been investigated by C. Buckley [Buckley 1985].

11. Real-Time Implementation

Finally, the global control system integrating the potential field concept with the operational space approach has the following structure:

$$\Gamma = \Gamma_{motion} + \Gamma_{obstacles} + \Gamma_{joint\ limit}; \quad (32)$$

where:

$$\Gamma_{motion} = J^T(q)\Lambda(q)F^*_{x_d} + \tilde{B}(q)[\dot{q}\dot{q}] + \tilde{C}(q)[\dot{q}^2] + g(q); \quad (33)$$

The control system architecture is shown in Figure 5 where np represents the number of PSP's. The Jacobian matrices $J^T_{psp_j}$ have common factors with the end-effector Jacobian matrix J^T. Thus, their evaluation does not require significant additional computation.

12. Applications

An experimental manipulator programming system COSMOS (Control in Operational Space of a Manipulator-with-Obstacles System), has been designed at the Stanford Artificial Intelligence Laboratory for implementation of the operational space control approach for the Unimation PUMA 560 arms. For these manipulators, the ability to control joint torque is considerably restricted by the nonlinearities and friction inherent in their joint actuator/transmission systems. Therefore, the centrifugal and Coriolis forces have been ignored in the PUMA end-effector dynamic model.

The COSMOS system is implemented on a PDP 11/45 interfaced to a PUMA 560. The PDP 11/23 and VAL are discon-

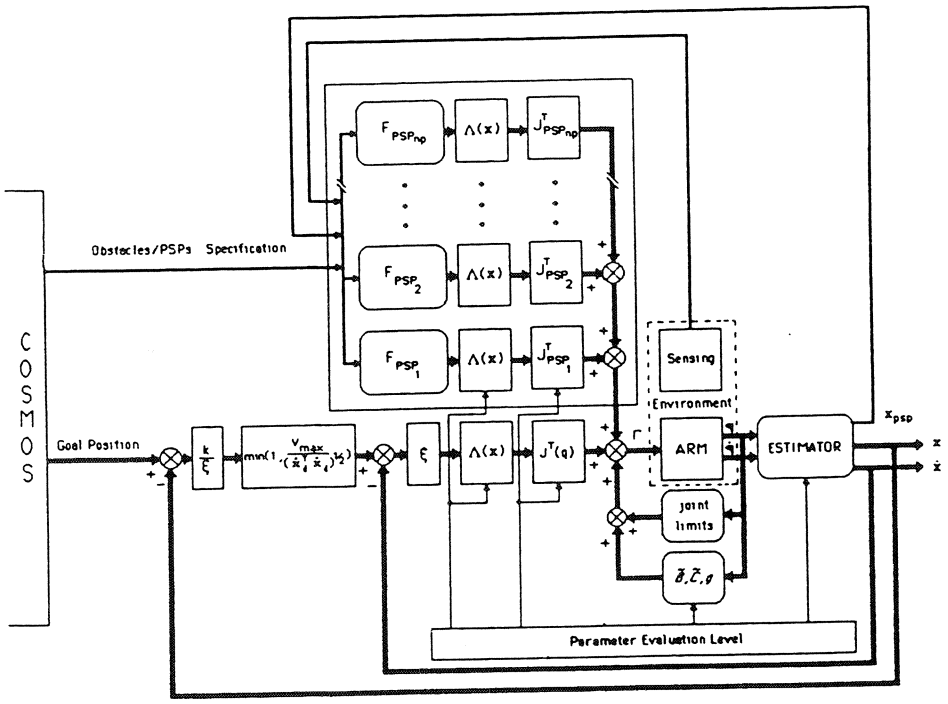

Figure 5. *Operational Space Control System Architecture.*

nected, and only the joint microprocessors in the PUMA controller are used for motor current control. The PUMA is equipped with a six degree of freedom wrist force, and two three degree of freedom finger force sensors. The PUMA is also interfaced to a Machine Intelligence Corporation vision module.

The rate of the servo control level is 125 Hz while the parameter evaluation level runs at 40 Hz. With the new multiprocessor implementation (PDP 11/45 and PDP 11/60), COSMOS has achieved a dynamic and kinematic update rate of 100 Hz and a servo control rate of 250 Hz.

We have demonstrated real-time end-effector motions both free and constrained, with the COSMOS system. These include contact, slide, insertion, and compliance operations, as well as real-time collision avoidance with links and moving obstacles [Brooks and Khatib 1984, Khatib 1985b].

13. Summary and Discussion

We have presented our operational space formulation of manipulator control which provides the basis for this obstacle avoidance approach, and have described the two-level architecture designed to increase the real-time performance of the control system. The operational space formulation has been shown to be an effective means of achieving high dynamic performance in real-time motion control and active force control of robot manipulators for complex assembly tasks. In addition, the complex transformation of the task into joint coordinates, required in conventional joint space control approaches, is eliminated.

Further, we have described the formulation and the implementation of a real-time obstacle avoidance approach based on the artificial potential field concept, using analytic primitives for obstacle geometric modelling. In this approach, collision avoidance, generally treated as high level planning, has been demonstrated to be an effective component of low level real-time control.

The integration of this low level control approach with a high level planning system seems to be one of the more promising solutions to the obstacle avoidance problem in robot control. With this approach, the problem may be treated in two stages:

- at high level control, generating a global strategy for the manipulator's path in terms of intermediate goals (rather than finding an accurate collision-free path);
- at the low level, producing the appropriate commands to attain each of these goals, taking into account the detailed geometry and motion of manipulator and obstacle, and making use of real-time obstacle sensing (low level vision and proximity sensors).

By extending low level control capabilities and reducing the high level path planning burden, the integration of this collision avoidance approach into a multi-level robot control structure will improve the real-time performance of the overall robot control system. Potential applications of this control approach include moving obstacle avoidance, grasping collision avoidance, and obstacle avoidance problems involving multi-manipulators with multi-fingered hands.

Acknowledgments

Tom Binford and Bernie Roth have encouraged and given support for the continuation of this research at Stanford University.

References

[Brooks 1983]
Brooks, R. 1983. Solving the Find-Path Problem by Good Representation of Free Space. IEEE Systems, Man and Cybernetics. SMC-13:190-197.

[Brooks 1984]
Brooks, R. 1984 (Aug. 20-23). Aspects of Mobile Robot Visual Map Making. Second International Symposium of Robotics Research. Kyoto, Japan.

[Brooks and Khatib 1984]
Brooks, K. and Khatib, O. 1984 (June). Robotics in Three Acts (Film). Stanford University.

[Buckley 1985]
Buckley, C. 1985. The Application of Continuum Methods to Path Planning. Ph.D. Thesis (in progress). Stanford University. Department of Mechanical Engineering.

[Chatila 1981]
Chatila, R. 1981. Système de Navigation pour un Robot Mobile Autonome: Modélisation et Processus Décisionnels. Thése de Docteur-Ingénieur. Université Paul Sabatier. Toulouse, France.

[Craig and Raibert 1979]
J.J. Craig, and M. Raibert, M. 1979. A systematic Method for Hybrid Position/Force Control of a Manipulator. Proceeding 1979 IEEE Computer Software Applications Albuauerque, Conference Chicago.

[Hogan 1983]
Hogan, N. 1984 (June 6-8). Impedance Control: An Approach to Manipulation. 1984 American Control Conference, San Diago.

[Khatib, Llibre and Mampey 1978a]
Khatib, O., Llibre, M. and Mampey, R. 1978. Fonction Decision-Commande d'un Robot Manipulateur. Rapport No. 2/7156. Toulouse, France. DERA/CERT.

[Khatib and Le Maitre 1978b]
Khatib, O. and Le Maitre, J.F. 1978 (September 12-15). Dynamic Control of Manipulators Operating in a Complex Environment. 3rd CISM-IFToMM. Udine, Italy.

[Khatib 1980]
Khatib, O. 1980. Commande Dynamique dans l'Espace Opérationnel des Robots Manipulateurs en Présence d'Obstacles. Thése de Docteur-Ingénieur. École Nationale Supérieure de l'Aéronautique et de l'Espace (ENSAE). Toulouse, France.

[Khatib 1983]
Khatib, O. 1983 (September 15-20). Dynamic Control of Manipulators in Operational Space. Sixth CISM-IFToMM Congress on Theory of Machines and Mechanisms. New Delhi, India.

[Khatib 1985]
Khatib, O. 1985 (March 25-28). Real-Time Obstacle Ovoidance for Manipulators and Mobile Robots. 1985 International Conference on Robotics and Automation. St. Louis.

[Khatib 1985b]
Khatib, O. 1985. Robotics in Three Acts - Part II (Film). Stanford University.

[Krogh 1984]
Krogh, B. 1984 (August). A Genralized Potential Field Approach to Obstacle Avoidance Control. Robotics Research: The Next Five Years and Beyond, SME Conference Proceedings, Bethlehem, Pennsylvania.

[Kuntze and Schill 1982]
Kuntze, H. B. and Schill, W. 1982 (June 9-11). Methods for Collision Avoidance in Computer Controlled Industrial Robots. 12th ISIR, Paris.

[Lozano-Perez 1980]
Lozano-Perez, T. 1980 Spatial Planning: A Configuration Space Approach. AI Memo 605. Cambridge, Mass. MIT Artificial Intelligence Laboratory.

[Moravec 1980]
Moravec, H.P. 1980. Obstacle Avoidance and Navigation in the Real World by a Seeing Robot Rover. Ph.D. Thesis. Stanford University. Artificial Intelligence Laboratory.

[Salisbury 1980]
Salisbury, J.K. 1980 (December) Active Stiffness Control of a Manipulator in Cartesian Coordinates. 19th IEEE Conference on Decision and Control, Albuauerque, New Mexico.